Chapter 8

Plant silicon isotopic signature might reflect soil weathering stage *

Abstract

Silicon isotopic data in plant and soil can readily contribute to the understanding of the Si continental cycle. Young banana plantlets (*Musa acuminata* Colla, cv Grande Naine) fractionate Si stable isotopes in hydroponics. Here we report on plant Si content and Si-isotopic fractionation in mature banana plants cultivated on soils differing in weathering stage, but all developed from basaltic pyroclasts in the Mungo area, Cameroon. The δ^{30}Si vs. NBS28 compositions were determined in various plant parts by MC-ICP-MS in dry plasma mode with external Mg doping with a precision below 0.15‰ ($\pm 2\sigma_{SD}$). Plant signatures confirmed the intra-plant fractionation of Si isotopes highlighted in hydroponics, and showed a trend similar to other plant species. The δ^{30}Si signatures were heavier in banana plants cultivated on weathered clayey soils (+0.54±0.15‰) than on weakly developed soils rich in fresh ash and pumice (+0.11±0.16‰), indicating a strong effect of the Si source. Plant Si isotopic signature might thus reflect the weathering stage of soils.

*Adapted from Opfergelt S., Delvaux B., André L., Cardinal D. Plant Si isotopic signature might reflect soil weathering stage. *Biogeochemistry*, under revision.
Preliminary results presented in Appendix C and D.
Complementary data in Appendix E

8.1 Introduction

Silicon plays a crucial role in global biogeochemical processes such as the regulation of carbon dioxide (Berner, 1997; Volk, 1987), the buffering of proton fluxes through silicate dissolution (Rai and Kittrick, 1989), and the nutrition of both marine and terrestrial biota (Smetacek, 1999). Since the rates of mineral dissolution can be enhanced by plant effects on silicate weathering (Moulton et al., 2000), plants can exert a strong imprint on the Si continental cycle (Alexandre et al., 1997; Conley, 2002; Derry et al., 2005). However, only few studies were carried out so far to quantify their contribution to the continental cycle of Si, and more specifically within the soil-plant system. The quantification of silicon isotopic fractionation by biotic and abiotic processes can readily contribute to the understanding of the continental cycle of silicon. These processes involve Si uptake by biota (De La Rocha, 2003; De La Rocha et al., 1997; Ding et al., 2003 2005b; Douthitt, 1982; Opfergelt et al., 2006b; Ziegler et al., 2005a)(Chapter 7), silicate weathering (Georg et al., 2006a 2007c; Ziegler et al., 2005ab), clay formation (Ziegler et al., 2005a), and silica adsorption on oxide surfaces (Chapter 10). They all imply a decrease of the δ^{29}Si and/or δ^{30}Si values in the biota-, clay- and oxide-compartments, thereby involving heavier Si-isotopic signatures in nutrient, equilibrium or drainage solutions (Opfergelt et al. (2006b); Ziegler et al. (2005a); Chapter 7; Chapter 10). The Si-isotopic signature of a given plant species or, better, cultivar, could thus be impacted not only by Si uptake, but also by soil weathering stage, which, indeed, results in the formation of both clay minerals and iron oxides (Bikerland, 1974).

We have recently shown that Si accumulation by young banana plantlets (*Musa acuminata* Colla, cv Grande Naine) in hydroponics is controlled by Si availability in the nutrient solution (Henriet et al., 2006), and involves a Si-isotopic fractionation between plant parts (Opfergelt et al. (2006b); Chapter 7). Here, we determine the first Si-isotopic compositions in mature banana plants (*Musa acuminata* Colla, cv Grande Naine) from root to fruit. We use banana plants cultivated on soils developed on basaltic pyroclasts, but differing in their weathering stage, and thus in their clay and oxide contents (Delvaux et al., 1989). Though derived from similar volcanic ash, these contrasted soils are thus here viewed as distinct Si sources.

8.2 Materials and methods

8.2.1 Study area

The study area lies in the Mungo plain in Cameroon, West Africa (Njombé-Penja-Loum, 4°30'-4°53'N 9°37'-9°50'E, 70km north of Douala). The climate is humid tropical: the rainy season extends from March to November with a total average annual rainfall of 2700 mm year^{-1}, and temperature varies with altitude between 22.4°C (870m) and 27.5°C (40m) (Martin and Sieffermann, 1966). The Mungo plain is a graben extending over 80 km on a south-west - north-east axis, covered by basaltic lava flows, ash and pumice deposits, which are Quaternary in age (early Quaternary to present times) (Nkouathio et al., 2002), part of the N30°E Cameroon Hot Line (Déruelle et al., 2007). The soils devoted to intensive banana cropping derive from the pyroclastic deposits in the altitude range 100-250m asl. The soils are members of a weathering sequence corresponding to the soil mineralogical sequence ash-allophane-halloysite-kaolinite: with increasing weathering stage, volcanic ash and glass content decreases whereas clay and free Fe oxide contents increase (Delvaux et al., 1989). The soils thus strongly differ in their mineralogical and physico-chemical properties despite of their similar parent rock, according to their weathering stage.

The Mungo area has long been affected to intensive banana cropping since the fifties of last century (Delvaux, 1988). The cropping systems are based on successive cycles of 7-9 months before harvesting. At harvesting time, banana leaves and pseudostems are cut and left on soil surface. Banana fields are irrigated during the dry season by surrounding river waters; fertilizers (N, P, K, Mg) are applied on a monthly basis whereas lime amendments (Ca) are applied on a two-years basis. Four stations were selected from poorly developped (PD) to strongly weathered (SW) volcanic soils (vs) composing the weathering sequence: Dia-Dia (DD), Sir (SR), Mbomé (MB), Djungo (DJ) from PDvs to SWvs, respectively. PDvs are rich in weatherable minerals and poor in clay (10-35%) containing allophane, halloysite and ferrihydrite. Oppositely, SWvs are fine clayey soils (70-96% clay), rich in halloysite, kaolinite, gibbsite and goethite (Delvaux et al., 1989 1990b).

8.2.2 Sampling

Banana plant parts (*Musa acuminata* Colla, cv Grande Naine) were sampled in each station (DD, SR, MB, DJ) in November 2005, at the end of the rainy season. In each station, five plants were selected at flowering stage according to the international foliar sampling procedure

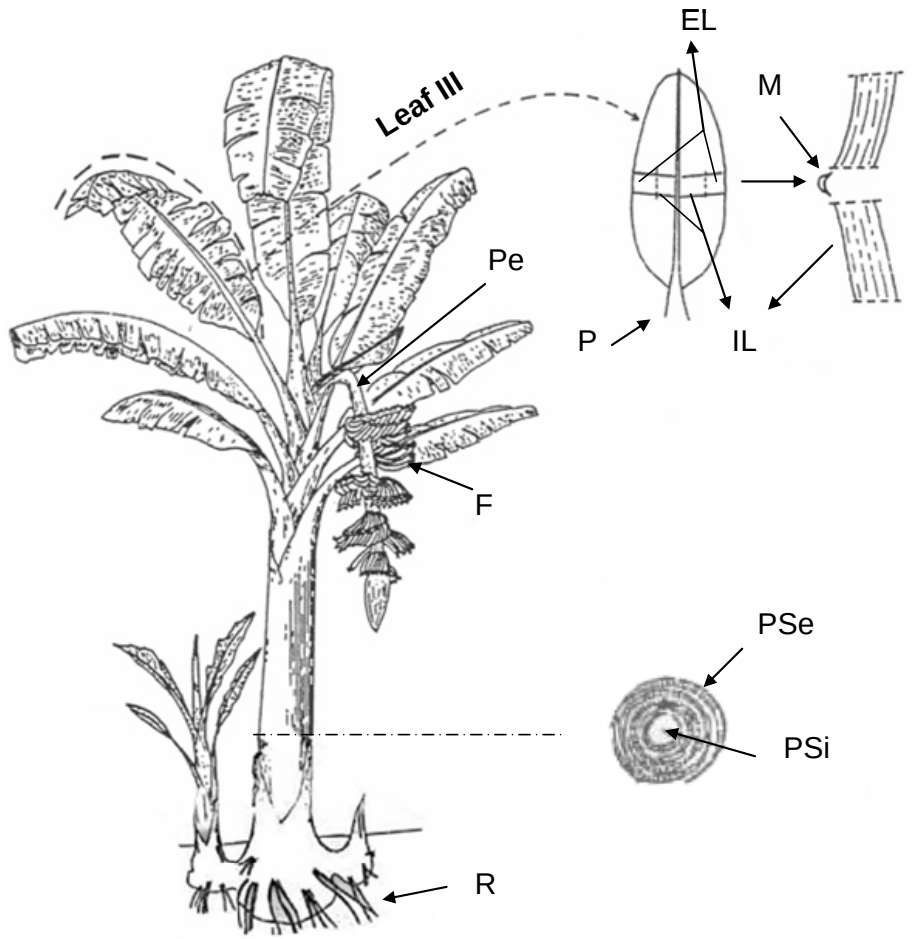

Figure 8.1: Schematic banana plant morphology at flowering stage: root (R), peduncle (Pe), fruit (F); cross section indicating internal (PSi) and external pseudostem (PSe); leaf III with petiole (P), midrib (M), internal lamina (IL), and external lamina (EL) (adapted from Champion (1963); Martin-Prével (1984)).

(Martin-Prével, 1984) involving the sampling of petiole (P), midrib (M), internal and external lamina (IL, EL) of leaf III (Figure 8.1). Among the five, one plant was sampled from root to fruit: root (R), internal pseudostem (PSi), external pseudostem (PSe), P, M, IL, EL, peduncle (Pe) and fruit (F) (Figure 8.1). The other four plants were used to build up four composite foliar samples (P, M, IL, EL). As the pseudostem is constituted of leaf sheaths, external sheaths corresponding to the oldest

leaves, we collected separately the external green sheaths (PSe) and the internal white sheaths (PSi) (Figure 8.1), considering a possible Si accumulation in external sheats related to leaf age and transpiration (Motomura et al., 2004). For the fruit, the middle fingers of the second hand were sampled.

Topsoils (00-05 cm) were sampled in each station 50 cm around each matt, after cleaning up the soil surface from banana litter residues. The topsoils were then mixed to build up a topsoil composite sample. Fresh pumice particles were collected in the flanks of the most recent volcanic cone in the Mungo plain (Mont Pelé).

Stream water used for both crop irrigation at Dia-Dia and Djungo station was sampled. Water sample was immediately filtered through 0.45μm polycarbonate membranes, acidified with suprapur HNO_3 and stored at fresh temperature in the dark, in acid-cleaned polypropylene bottle.

8.2.3 Bulk elemental, chemical and physical analyses

The dry weight of plant materials from the four stations (DD, SR, MB, DJ) was determined after drying all plant parts at 60°C for one week. Elemental analysis was carried out after borate fusion at 1000°C and dissolution of fusion beads in 10% HNO_3 (Chao and Sanzolone, 1992). The concentrations of Si, Al, Ca, Mg and K were determined by inductively coupled plasma atomic emission spectrometry (ICP-AES); the detection limit for Si in solution was 0.7 μM Si.

The soil samples were air dried at room temperature during 24 h, and sieved at 2mm. Elemental analysis was carried out after calcination and Li-metaborate and Li-tetraborate fusion (Chao and Sanzolone, 1992). Briefly, a crushed sample of 100 mg was melted at 1000 °C for 5 minutes in a graphite crucible in the presence of 0.4 g Li-tetraborate and 1.6 g Li-metaborate. The cooled melt was then dissolved in 200 ml of 2 M HNO_3 under magnetic agitation at 90-100°C. The contents of Si, Al, Fe, Ca, Mg, K were determined by ICP-AES. The total contents of alkaline and alkaline-earth cations were summed up as the total reserve in bases (TRB), which estimates the content of weatherable minerals in mineral soil horizons (Herbillon, 1986). The content of free iron oxide was determined after selective dissolution of Fe oxide in the Na-dithionite-citrate-bicarbonate (DCB) extract (Mehra and Jackson, 1960). The ratio of DCB-extractable Fe over total Fe content (Fe_d/Fe_t) is an index of soil weathering stage, just as TRB and clay content (Delvaux et al., 1989). The particle size distribution was determined by quantitative

recovery of clay, silt and sand fractions after sonication and dispersion with Na^+-saturated resins (Bartoli et al., 1991; Rouiller et al., 1972).

8.2.4 Silicon isotopes analyses

The Si isotopic composition was measured: (1) both in the soil samples (<2mm) and clay fractions (<2μm) from the four stations (DD, SR, MB, DJ), (2) in the fresh pumice material (3) in the irrigation water and (4) in plant materials from two selected stations (DD, DJ), in order to compare two contrasted Si sources: the weakly developed PDvs (DD) *versus* the strongly weathered SWvs (DJ).

From soil and clay samples, silicon was recovered from each aliquot by alkaline fusion at 1000°C of 5mg of silicate powder mixed with 30mg of $LiBO_2$ flux in a covered Pt crucible and dissolution in double distilled 5% HNO_3 (Abraham et al. (2008); Chapter 5). From plant aliquot, silicon was recovered after: (1) mineralization at 450°C during 24 hours in Pt crucibles, (2) opal dissolution by 0.2 M NaOH leaching at 100°C during 2 hours (adapted from Ragueneau et al. (2005)).

Dissolved Si from soil, plant and water samples was purified by triethylamine molybdate (TEA-moly) co-precipitation and combustion in covered Pt crucibles at 1000°C (De La Rocha et al., 1996), and dissolved in dilute suprapur HF-HCl mixture (Cardinal et al., 2003).

The Si-isotopic compositions in soil, clay, pumice and plant samples were measured using a Nu Plasma multicollector plasma source mass spectrometer (MC-ICP-MS) operating in dry plasma mode, with an external Mg doping to correct mass bias (Cardinal et al., 2003). To avoid matrix effects, purity of the samples (absence of major elements and Mo) was controlled by ICP-AES before MC-ICP-MS analyses. Data were obtained by the sample-standard bracketing technique relative to the NBS28 silica sand standard (National Institute of Standard and Technology RM #8546) for silicon isotopes. The analytical method was supported by an inter-laboratory comparison exercise and proved to be accurate on secondary reference materials (Reynolds et al. (2007); Chapter 6). A new method solving the isobaric interference of $^{14}N^{16}O$ on ^{30}Si was developed (Abraham et al. (2008); Chapter 5). Previously, only ^{29}Si:^{28}Si ratios were accurately measured. In this study, our results were expressed as $\delta^{30}Si$ vs. NBS28 (‰) with an average precision and accuracy below 0.15‰ ($\pm$ $2\sigma_{SD}$) following:

$$\delta^{30}Si = \left[\frac{\left(\frac{^{30}Si}{^{28}Si}\right)_{sample}}{\left(\frac{^{30}Si}{^{28}Si}\right)_{NBS28}} - 1 \right] \times 1000$$

The data obtained as δ^{29}Si values were converted to δ^{30}Si values by using the multiplying factor 1.93 assuming a mass-dependent fractionation process (Young et al., 2002) following the equilibrium fractionation law. This is supported by equilibrium fractionation processes observed in natural rivers (Georg et al., 2006a 2007c).

8.3 Results

8.3.1 Soil properties

Table 8.1 presents the soil data. These data are strongly consistent with the increase of soil weathering stage from DD to DJ, as previously reported for this weathering sequence (Delvaux et al., 1989). Indeed, TRB decreases with increasing values of both the clay content and Fe_d/Fe_t ratio, meaning that the dissolution of primary weatherable minerals resulted in the synthesis of clays and iron oxides. In this respect, DD (PDvs) and DJ (SWvs) strongly differ in soil weathering stage, as they exhibit contrasting TRB values (703 *vs* 183 $cmol_c\ kg^{-1}$) and clay contents (25 *vs* 72%). In DD, 22% of Fe is allocated to free oxide *vs* 78% to Fe-silicate against 60% of Fe as free oxide in DJ.

Table 8.1: Characteristics of the topsoils (0-5cm): Total Reserve in Bases (TRB), DCB-extractable Fe content over total Fe content (Fe_d/Fe_t), and clay content.

Station	TRB $cmol_c\ kg^{-1}$	Fe_d/Fe_t	Clay content %
Dia-Dia	703	0.22	25
Sir	469	0.36	42
Mbomé	323	0.40	58
Djungo	183	0.60	72

Si-isotopic data are presented in Table 8.2. The δ^{30}Si value determined in the fresh pumice material can be considered as the Si-source value (-0.38‰). With respect to this value, δ^{30}Si was similar in the PDvs at DD (-0.41‰), but much lighter in the SWvs DJ (-1.41‰). As expected (Ziegler et al., 2005b), the δ^{30}Si values decrease in the respective clay fractions of PDvs DD (-1.19‰) and SWvs DJ (-2.37‰) as well as with increasing soil weathering stage, DJ being much more

weathered than DD. Stream water used for crop irrigation display a positive isotopic signature (+1.35‰) which is in the range of signatures of rivers (Alleman et al., 2005; De La Rocha et al., 2000; Ding et al., 2004).

Table 8.2: δ^{30}Si values of the topsoil (<2mm; n=2) and clay (<2μm; n=1) samples, as compared to δ^{30}Si value of fresh pumice material (n=2). δ^{30}Si value of the stream water used for crop irrigation (n=1).

Station	Soil * δ^{30}Si (‰)	Clay δ^{30}Si (‰)	Pumice * δ^{30}Si (‰)	Water * δ^{30}Si (‰)
Mont Pelé	-	-	-0.38	-
Dia-Dia	-0.41	-1.19	-	-
Djungo	-1.41	-2.37	-	-
Irrigation water	-	-	-	+1.35

* δ^{30}Si calculated from δ^{29}Si measured using factor 1.93

8.3.2 Mineral content in plants

Table 8.3 presents the contents of Ca, Mg, K, Al in the internal lamina (IL) of leaf III, and Al content of roots, as determined in the samples collected in the four stations DD, SR, MB, DJ. The foliar IL Ca content decreases from DD to DJ compared to K content. This supports that the nutritional status of banana plants is strongly governed by soil weathering stage in this area because PDvs are rich in Ca-bearing primary minerals, and SWvs selectively sorb K^+ ions on their clay surfaces, thereby contributing positively to the storage and bioavailability of potassium (Delvaux et al., 1990a 1989). Al content in roots is substantial compared to Al content in IL (Table 8.3). The contribution of Al^{3+} adsorbed onto root surfaces is likely negligible at soil pH above 7, as measured in these soils, despite the fact that proton extrusion by banana roots may decrease pH in the surrounding environment and mobilize Al from mineral dissolution (Rufyikiri et al., 2004). Here, we consider that root-Al (Table 8.3) is in fact a signature of clay minerals adhering to root surfaces, and that these clay minerals are dominantly phyllosilicates exhibiting a 1:1 Si:Al atomic ratio (Delvaux et al., 1990b). We thus correct the Si content of banana roots accordingly.

Figure 8.2 illustrates the bulk Si contents in the various plant parts collected at the four stations. Si content in roots ranges between 0.2 and

Table 8.3: Al content in root and Ca, Mg, K and Al content and K/Ca ratio within internal lamina (IL) through the weathering sequence. DL = detection limit.

Station	Ca %	Mg %	K %	K/Ca $cmol_c.kg^{-1}$	Al %	Al[a] %
Dia-Dia	0.81	0.29	3.82	2.41	0.006	0.15
Sir	0.61	0.21	4.73	3.97	<DL	0.09
Mbomé	0.61	0.25	4.33	3.66	<DL	0.07
Djungo	0.45	0.28	4.01	4.52	<DL	0.05

[a] Al in roots

0.4 % after Si:Al correction. Si content in banana shoots ranges between 0.1 and 0.9 %. The largest Si content was recorded in the external green sheaths of the pseudostem (PSe). In banana leaves, the concentration of Si follows a gradient from the petiole (P) to the external lamina (EL) from 0.1 to 0.7 %Si. The Si concentration ranges between 0.3 to 0.5 % in the peduncle (Pe), and between 0.1 to 0.2 % in the fruit.

8.3.3 Silicon isotopic compositions in plants

Table 8.4 and Figure 8.3 give the isotopic compositions in the plant parts from the two contrasted stations DD (PDvs) and DJ (SWvs). The Si-isotopic composition measured in banana roots has been corrected for clay contribution as discussed above and assuming a clay isotopic composition δ^{30}Si of -1.19 and -2.37‰ as measured in DD and DJ clay samples, respectively (Table 8.2). The corrected root Si-isotopic signatures are slightly heavier than the ones determined in the internal pseudostem, in good agreement with the Si-isotopic compositions of young banana roots as measured in hydroponics (Opfergelt et al. (2006b); Chapter 7) which strengthens the validity of our correction (Figure 8.3).

Silicon isotopic compositions in various plant parts (δ^{30}Si values at DD and DJ) range between -0.18 and +1.09‰ showing a clear trend from lighter to heavier Si-isotopic composition from pseudostem to fruit (Figure 8.3). This trend is similar in both stations, at Dia-Dia and Djungo.

The bulk plant isotopic composition is calculated just like for rice in Ding et al. (2005b), by balancing the Si-isotopic composition of each plant part by the Si proportion of each plant part in the total plant Si content (Table 8.4). Si proportion of each plant part is calculated using the Si content measured in this study and the biomasses measured by Martin-Prével and Montagut (1966) in each respective plant part

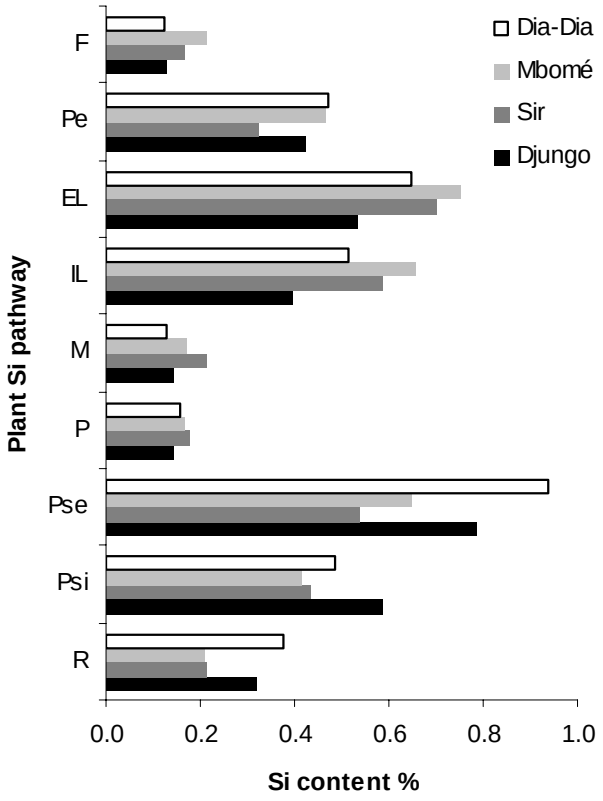

Figure 8.2: Si content in banana plant parts collected in the four stations DD, SR, MB, DJ. R = roots ; Psi, PSe = internal and external pseudostem; P = petiole; M = midrib ; IL, EL = internal and external lamina ; Pe = peduncle; F = fruit.

of banana (roots were excluded from this calculation as no biomass data were acquired). The computed bulk plant isotopic composition is clearly heavier at Djungo (δ^{30}Si = +0.54±0.15‰) than at Dia-Dia (+0.11±0.16‰) (Table 8.4).

8.4 Discussion

8.4.1 Silicon content in banana

Si contents in mature banana plants are similar to the ones measured in young banana plantlets grown in hydroponics (0.05 and 1.3 %Si), in which they varied depending on the Si concentration in the nutrient solution ranging between 0.08 and 1.66 mMSi (Henriet et al., 2006).

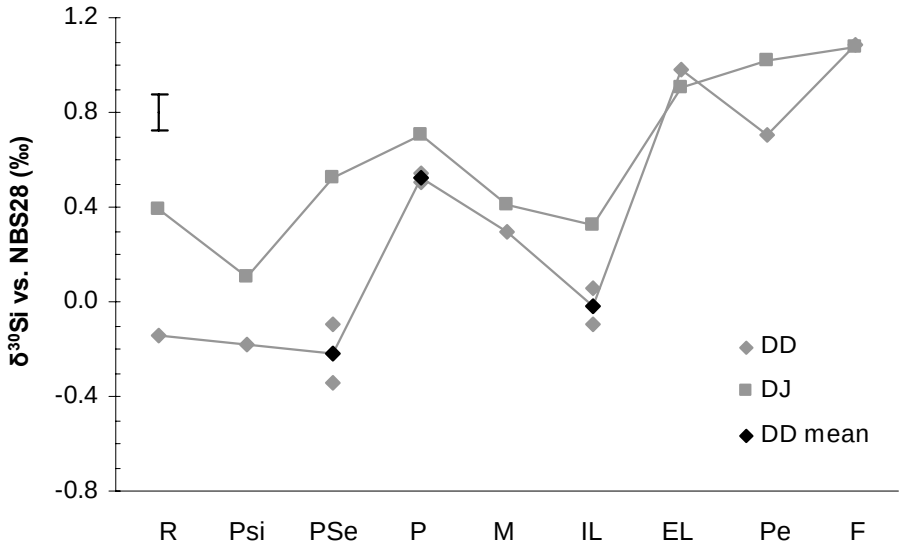

Figure 8.3: Si-isotopic compositions of various plant parts at Dia-Dia and Djungo. Bracket shows the standard error ($\pm\ 2\sigma_{SEM}$). R = roots ; PSi, PSe = internal and external pseudostem; P = petiole; M = midrib ; IL, EL = internal and external lamina ; Pe = peduncle; F = fruit.

This concentration falls within the range of Si concentrations in soil solution, varying between 0.01 and 1.99 mMSi (Karathanasis, 2002), and most commonly between 0.1 and 0.6 mMSi (Faure, 1991). The highest Si content recorded in the pseudostem confirms the results of Jauhari et al. (1974). The difference in Si contents between PSi and PSe can be related to the ageing of leaf tissues (Motomura et al., 2004), leading to a larger Si accumulation in older sheaths. The gradient of Si concentration in leaves from petiole to external lamina is similar to the one observed in juvenile banana plantlets from the same cultivar (Henriet et al., 2006) as well as in mature plants representing sixty one species and varieties of *Musa* spp. from the World *Musa* Collection of the Centre Africain de Recherches sur Bananiers et Plantains (CARBAP), Njombé, Cameroon (Henriet, 2008). This gradient is governed by the transport and accumulation of Si in major plant transpiration termini (Raven, 1983). The rather low content of Si in banana fruit (0.02%) confirms the previous data reported by Powell et al. (2005).

Table 8.4: Si-isotopic compositions of the different plant parts. The bulk plant isotopic composition is balanced by the Si content of each plant parts. PSi, PSe = internal and external pseudostem; P, M = petiole and midrib; IL, EL = internal and external lamina, Pe = peduncle, F = fruit.

Plant Part	Mass fraction [a] % total mass	Si content % dw	Si [b] % mass fraction	Si [c] % total	δ^{29}Si ‰	δ^{30}Si [d] ‰
Dia-Dia						
PSi	7.4	0.48	3.6	0.06	-0.09	-0.18
PSe	39.4	0.94	36.9	0.64	-0.05	-0.10
P, M	8.4	0.14	1.2	0.02	+0.22	+0.42
IL, EL	20.2	0.58	11.7	0.20	+0.27	+0.52
Pe	2.6	0.47	1.2	0.02	+0.36	+0.70
F	22.0	0.12	2.7	0.05	+0.56	+1.09
				Bulk Plant		**0.11**
Djungo						
PSi	7.4	0.58	4.3	0.09	+0.05	+0.10
PSe	39.4	0.79	30.9	0.62	+0.27	+0.52
P, M	8.4	0.14	1.2	0.02	+0.29	+0.56
IL, EL	20.2	0.46	9.4	0.19	+0.32	+0.62
Pe	2.6	0.43	1.1	0.02	+0.53	+1.02
F	22.0	0.13	2.8	0.06	+0.56	+1.08
				Bulk Plant		**0.54**

[a] calculated from Martin-Prével and Montagut (1966)
[b] Si (% mass fraction) = mass fraction × Si content
[c] Si (% total) = Si (% mass fraction)/ $\sum$ Si (% mass fraction)
[d] calculated from δ^{29}Si measured using factor 1.93

8.4.2 Intra-plant silicon isotopic fractionation

Mature banana plants present heavier Si-isotopic compositions in the upper shoots than in the pseudostem, corroborating the trend previously reported for the same variety in hydroponics (Opfergelt et al. (2006b); Chapter 7). This experimental convergence strengthens the validity of our plant-source fractionation factor determined experimentally in hydroponics. It underlines also that juvenile banana plantlets in hydroponics, and mature banana plants in field conditions behave with similar dynamics of Si isotopic mass fractionation. The trend is, moreover, similar in mature banana plants cultivated on two contrasted soils (DD and DJ), as illustrated in Figure 8.3. The first Si-isotopic signatures of banana peduncle and fruit are provided here. These two ultimate Si pools were isotopically heavier than the other parts of the shoots, which is in very good agreement with the general intra-plant trend.

Si-isotopic data in plants are scarce. Here, we compare our Si-isotopic data on banana (*Musa acuminata* Colla, cv Grande Naine; Opfergelt et al. (2006a); Appendix C; this study) with published data obtained for three other plant species: rice (*Oryza* sp.; Ding et al. (2005b)), bamboo (*Bambusa* sp.; Ding et al. (2003); Douthitt (1982)),

horsetail (*Equisetum* sp.; Douthitt (1982)) (Figure 8.4).

The available δ^{30}Si values of phytoliths in various plant species range between -2.2 and +6.1‰ (Figure 8.4). There is a general trend revealing lighter to heavier isotopic composition from stem to leaf, indicating a homogeneous intra-plant Si isotopic fractionation process within three plant species: banana (this study), rice (Ding et al., 2005b) and bamboo (Ding et al., 2003). This suggests that the Si isotopic composition of phytoliths depends on their precipitation locus. However, the Si-isotopic range in banana is narrower than the one observed in rice and bamboo (Figure 8.4) and there is a difference between DD and DJ (Figure 8.3). As discussed below, this might be attributed to (i) a difference in Si accumulation among plant species, (ii) a different physiological stage, (iii) a difference between Si sources from soils.

(i) Rice and bamboo accumulate much more Si on a dry weight basis (up to 4.7% in rice: Ding et al. (2005b); 3.3% in bamboo: Ma and

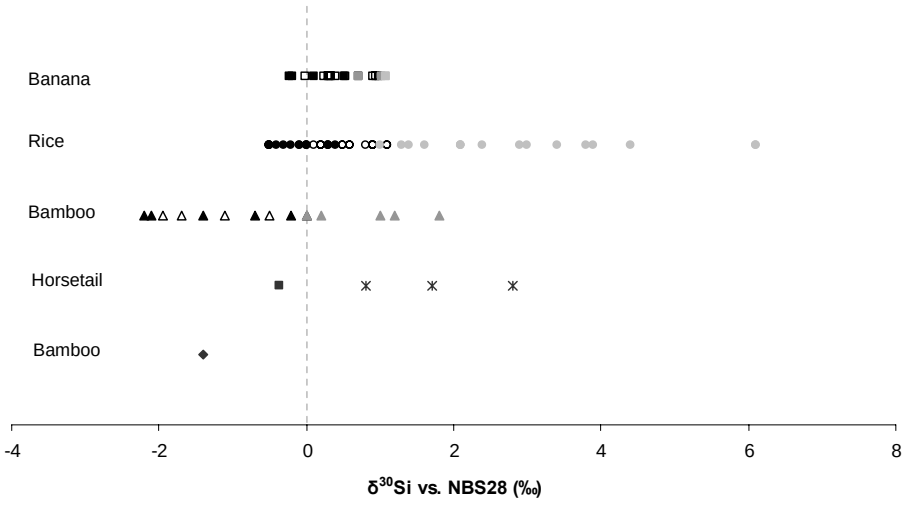

Figure 8.4: Si-isotopic compositions in various plant species: (1) banana (*Musa acuminata* Colla, cv Grande Naine; Opfergelt et al. (2006a); Appendix C; this study); (2) rice (*Oryza* sp.; Ding et al. (2005b)); (3) bamboo (*Bambusa* sp.; triangle, Ding et al. (2003); diamond, Douthitt (1982)); (4) horsetail (*Equisetum* sp.; stars, Douthitt (1982); square, unpub. data, S. Opfergelt). Detailed isotopic compositions of plant parts are indicated by black, open and grey dots, respectively, when available: banana (pseudostem, leaf, peduncle-fruit, respectively), rice (stem-leaf, husk, grains, respectively), bamboo (stem, branch, leaf, respectively).

Takahashi (2002)) than do the banana plants analysed in this study (0.9%). The density of Si transporters should differ between plant species, and may thus impact plant Si accumulation (Ma and Yamaji, 2006). In rice plant, Si uptake by roots is mediated by an influx and an efflux transporter (Ma et al., 2006 2007). These transporters might be responsible for Si isotopic fractionation between plant parts in banana (Opfergelt et al. (2006b); Chapter 7). We therefore suggest that the extent of the isotopic fractionation factor might differ between vegetal species in relation to the density of Si transporters in plants.

(ii) Here, banana plants were collected at flowering stage whereas rice plants were sampled at harvesting stage (Ding et al., 2005b). A likely higher Si accumulation at this stage would have probably induced a larger isotopic fractionation in rice plant.

(iii) Si source from soil solution would definitely impact the bulk plant isotopic compositions. Yet, no information about the source is available for the data on rice and bamboo considered in Figure 8.4. In the present study, the Si source could have impacted the isotopic fractionation of Si in the banana plants sampled at DD and DJ, since the plant physiological stage and Si content do not differ between the sites. We develop this hypothesis here below.

8.4.3 Plant silicon isotopic signature might reflect soil weathering stage

Confirming previous studies (Delvaux, 1988; Delvaux et al., 1989), our bulk analytical data show that DD and DJ stations clearly correspond to, respectively, weakly developed soils rich in volcanic glass (PDvs), and weathered clayey soils rich in secondary phyllosilicates, Fe and Al oxides (SWvs). Banana plants are isotopically heavier on the most weathered soil considered here (δ^{30}Si = +0.54‰ at DJ against +0.11‰ at DD). This might be similar to bamboo, for which higher δ^{30}Si values were measured in plants grown in "mature garden" soil compared to "immature soil" (Ding et al., 2003). The heavier Si isotopic signature in banana plants cropped at DJ might result from a heavier Si source in the soil solution, which might result in turn from a combination of different processes. The Si source could be estimated by applying the plant-source fractionation factor measured experimentally ($^{30}\varepsilon$ = -0.77‰; Opfergelt et al. (2006b); Chapter 7) to the bulk plant isotopic compositions reported in the present study.

$$\delta^{30}Si_{source} = \delta^{30}Si_{bulk\ plant} - {}^{30}\varepsilon$$

Applying this equation would give a computed δ^{30}Si value for the Si source of +0.88‰ at Dia-Dia, and of +1.32 ‰ at Djungo. This would indicate that the Si source available for plants at Djungo is relatively strongly depleted in Si light isotopes.

Both the DD and DJ cropping areas are supplied by a unique source of irrigation water (δ^{30}Si = +1.35‰; Table 8.2). Consequently, a heavier soil solution at DJ could not be accounted for any difference in the isotopic composition of the waters supplied at DD and DJ. So the observed contrast in the plant Si isotopic compositions would likely reflect some soil-related mineralogical control. Two mechanisms can be invoked. (i) A Si isotopic fractionation induced by the synthesis of clay minerals, forming lighter clay minerals in the weathered soil SWvs compared to the weakly developed soil PDvs (Ziegler et al., 2005b) (Table 8.2): this process would deplete the soil solution in lighter Si isotopes. (ii) A preferential adsorption of light Si isotopes onto iron oxides (Chapter 10, 11), which are much more abundant in the clayey weathered soil SWvs (Table 8.1). These two abiotic processes may produce additive effects to control the Si-isotopic composition of the soil solution, and thereby the Si plant isotopic signature.

Compared to Dia-Dia, the SWvs at Djungo contains much more clay and iron oxide than the PDvs (Delvaux et al., 1989) (Table 8.1). The formation of clay minerals lighter at DJ (-2.37‰) than at DD (-1.19‰) would thus yield a heavier soil solution at DJ. In the PDvs DD, the isotopic signature of the Si source would be essentially controlled by the weatherable minerals massively present in the parent ash and pumice particles (δ^{30}Si = -0.38‰; Table 8.2), since the reserve in readily weatherable lithogenic silicates directly controls the Si soil-to-plant transfer (Henriet, 2008). This suggestion is supported by the lighter Si isotopic source value computed here above ($\delta^{30}Si_{source}$ = +0.88‰ at DD against +1.32 ‰ at DJ). A similar control of the Si isotopic signature by clay formation was observed in Iceland river waters (Georg et al., 2007c). Relatively lighter δ^{30}Si were measured in waters oversaturated in cations from basalt weathering. On the opposite, river waters undersaturated in these cations were isotopically heavier as a result of clay neoformation.

The heavier bulk plant δ^{30}Si at Djungo might thus be due to a heavier soil solution resulting from: (i) a high clay content linked to the strong weathering stage of the soil, and (ii) an adsorption of silica onto Fe oxides. In this respect, we thus believe that plant Si isotopic signature might reflect the weathering stage of soils.

8.5 Conclusion

Mature banana plants readily fractionate Si stable isotopes, like young banana plantlets cultivated in hydroponics (Opfergelt et al. (2006b); Chapter 7). The intra-plant trend in banana is similar to that observed in rice and bamboo. This similarity suggests that terrestrial plants may impact the Si isotopic budget at continental scale.

Moreover, the Si isotopic plant signature differs between soils depending on weathering stage. The relatively light and heavy plant isotopic signatures, as measured, respectively, at the weakly developed and the weathered soil, might result from clay accumulation and silica adsorption in the latter. Since both the contents of clay minerals and iron oxides increase with weathering, we conclude that plant Si isotopic signature might reflect soil weathering stage.